



Enhancing energy harvesting performance of bilayered parylene triboelectric nanogenerators through interfacial polarization

Minsoo P. Kim^{a,b,1}, Gunoh Lee^{c,1}, Byeongil Noh^c, Jaehyun Kim^c, Min Sub Kwak^a, Kyung Jin Lee^{c,*}, Hyunhyub Ko^{a,*}

^a School of Energy and Chemical Engineering, Ulsan National Institute of Science and Technology (UNIST), Ulsan, Republic of Korea

^b Department of Chemical Engineering, Suncheon National University, Suncheon, Republic of Korea

^c Department of Chemical Engineering and Applied Chemistry, College of Engineering, Chungnam National University, Daejeon, Republic of Korea

ARTICLE INFO

Keywords:

Triboelectric Nanogenerator
Bilayered structure
Interfacial polarization
Parylene
Carbon nanotube

ABSTRACT

Self-powered multifunctional devices have found applications in various fields including internet of things, smart robotics, and wearable haptic technologies. Triboelectric Nanogenerators (TENGs) are particularly noteworthy as they operate based on simple triboelectrification between contacting materials, and provide significantly higher output performance compared to other energy harvesting devices. In this study, we introduce soft bilayer structured films to significantly enhance the interfacial polarization and the resulting triboelectric output performance. The soft bilayer film is composed of two layers: a layer of parylene derivatives with different functional groups and a composite layer of polydimethylsiloxane (PDMS) embedded with multi-wall carbon nanotube (MWCNT). The parylene-deposited MWCNT-PDMS films effectively induce interfacial polarization due to the difference in permittivity between the parylene derivatives and MWCNT-PDMS, resulting in substantial improvement in triboelectric performances. Moreover, the specific functional groups present in the parylene monomers significantly affect the triboelectric polarity of the parylene-deposited bilayer films. The bilayer films deposited with parylene including fluorine, methyl hydroxyl, and hydroxyl groups, which improve the electron-withdrawing capability, exhibit negative triboelectric properties. In contrast, the bilayer film deposited with parylene including methyl amine group, which enhances the electron-donating ability, exhibits a positive triboelectric property. Owing to the highly improved interfacial polarization in the parylene-deposited bilayer films, our TENG consisting of paired bilayer films demonstrates superior output performance (4.57 W/cm² and 10.28 W/cm² for contact and separation step, respectively) compared to devices based solely on single layers of parylene- or PDMS (less than a few of mW/cm²). Our approach to designing layer-structured dielectric films offers a simple yet effective method to significantly enhance the output performance of self-powered flexible devices through improved polarization.

1. Introduction

Recently, the interest and research in multifunctional electronic devices have significantly grown, spanning a variety of fields such as the internet of things, smart robotics, and wearable haptic applications [1–3]. These devices essentially operate on external power sources like batteries, which have limited capacity and require regular recharging or replacement process. Consequently, the use of these devices in above-mentioned applications, where reliable and seamless operation is required, has faced restriction. To address these issues, energy

harvesting devices to convert ambient mechanical energy into electricity though a range of mechanisms [4] have been developed, making them well-suited for self-powered electronic systems. Among various types of energy harvesting devices, the triboelectric nanogenerators (TENGs) have garnered particular attention due to their attractive merits, including the availability of numerous accessible materials, simple device design, and a low-cost manufacturing process [5], which can be utilized in various fields such as self-powered wireless technology, smart-textile, human-machine interface, and biomedical applications [6–9]. TENGs operate through the process of triboelectrification of

* Corresponding authors.

E-mail addresses: kjlee@cnu.ac.kr (K.J. Lee), hyunhko@unist.ac.kr (H. Ko).

¹ These authors are equally contributed.

dissimilar contact-pair materials, leading to higher output performance compared to other energy harvesting devices. In terms of the working mechanism of TENGs, one of key factors that contribute to enhancing output performance is increasing the surface charge density of the materials involved in triboelectrification.

In triboelectric nanogenerators, surface charges are generated through the triboelectrification that occurs when triboelectric materials come into contact. During the separation process, opposite charges are induced and transferred to the electrodes via electrostatic induction, resulting in current flow through the external circuit. Consequently, most of researches have been focused on developing techniques to enhance surface charge density [10–18]. Surface modification techniques such as surface treatment involving the introduction or injection of single molecules with high electronegativity [10], and morphological engineering, which includes the control of surface patterns and roughness to increase the contact area [11], have been studied extensively. However, such approaches have inherent limitations in increasing the surface charge density, mainly due to the upper limit on electronegativity of materials or complicated patterning process. Another approach is the manipulation of dielectric polarization [12]. Tuning dielectric polarization can augment the surface charge density, which can be achieved through the addition of high-permittivity materials [13,14], stacking layers of dissimilar materials [15], or adjusting the dipole moment by controlling the chemical structures [16]. Heterogeneous composite films that incorporate high-permittivity nanoparticles into polymers are frequently used to boost the dielectric constant [13,17,18]. This enhancement is attributed to both the high-permittivity nanoparticle itself and the interfacial polarization, which occurs at the interface between the nanoparticle and the polymer matrix, subsequently leading to an increase in surface charge. However, it is important to note that the dielectric constants of these composite films have an upper limit that is lower than that of the nanoparticles themselves. Furthermore, the excessive addition of nanoparticles can actually impede the output performances, despite the increased dielectric constant. This counterproductive effect is attributed to the reduction in surface contact area due to the protrusion of nanoparticles [13]. An alternative approach involves manipulating the structures of polymer chains to enhance the dielectric constant and consequently improves the triboelectric performance [16]. However, this method typically involves complex synthesis process.

Unlike heterogeneous composite films, stacking dissimilar layers with large differences in permittivity and conductivity on the surfaces of electrodes is more effective in enhancing dielectric properties [19]. The mismatch in dielectric properties between the layers of triboelectric materials results in increased charge generation and polarization, known as interfacial polarization, during the triboelectric process, which, in turn, enhances the surface charge density and consequently improves the triboelectric performance [20]. Recently, our group has employed multilayer films as negative triboelectric layers [21]. By stacking dissimilar layers with mismatch in permittivity and conductivity, we have been able to effectively induce interfacial polarization, resulting in a higher dielectric constant than that of single layers, which subsequently enhances the surface charge density and triboelectric performance. For example, an elastic bilayer film consisting of a fluorinated polymer and soft PDMS demonstrates an increase in dielectric constant, leading to the highest output performance when compared to the PDMS-based triboelectric devices. Furthermore, ferroelectric multilayer nanocomposites consisting of alternating layers of poly(vinylidene fluoride-co-trifluoroethylene) (PVDF-TrFE) and BaTiO₃ nanoparticle (BTO NP) exhibit improved dielectric constants and resultant triboelectric performance in comparison to pure PVDF-TrFE and PVDF-TrFE/BTO nanocomposites. While films with a layer-stacking structure show promise as triboelectric materials for significantly enhancing triboelectric output performances through effective interfacial polarization, there are still issues that need to be addressed, such as (1) sensitivity to environmental factors such as

moisture, dust, and chemicals, and (2) control of film thickness at the nanoscale and (3) optimizing the conformal coating process to effectively induce interfacial polarization.

Poly(*p*-xylylene) derivatives, commonly referred to as parylene, are employed in a wide range of electronic devices because of their exceptional chemical and physical properties, such as excellent barrier properties, chemical stability, and defect-free conformal coating [22,23]. Additionally, unlike traditional triboelectric films, which are usually fabricated using conventional coating methods such as spin-coating, bar-coating, and spray-coating, parylene derivatives can be prepared with a controlled nanoscale thickness using chemical vapor deposition (CVD) at room temperature, leading to the uniform and conformal surface coatings. Furthermore, the incorporation of charged parylenes, such as the halogenated parylenes (e.g. Parylene C or AF₄), formylated-parylene, or aminated parylene, into the triboelectric films is beneficial to improving the triboelectric performances because of the charge-trapping capability arising from the reduction of electrical discharge due to their excellent barrier properties [23–25] as well as waterproof and thermal stability [26–29]. However, even with these enhancements, the output performance remains relatively low (less than tens of $\mu\text{W}/\text{cm}^2$, Table S1).

Given the aforementioned advantages of parylene, it is expected that triboelectric devices with layer-structured films incorporating parylene derivatives will demonstrate significantly improved output performance. When parylene materials incorporating different functional groups such as fluorine, hydroxyl, and amine are deposited on a surface, the resulting parylene-layered films can be utilized in various fields including flexible energy harvesting [25,30–36] and biological applications [26–29]. The incorporation of polar groups into the parylene units allows the dipole moment to be controlled, which, in turn, influences the dielectric constant, affecting the performance of triboelectric devices [16]. Despite the use of various parylene derivatives in triboelectric devices, which have shown a range of output performances [24,25,30,32,34,36], engineering dielectric materials within these devices to achieve high output performances remains a challenge.

In this study, we show that soft bilayer films composed of MWCNT-PDMS composites and parylene derivatives with various functional groups can significantly enhance the triboelectric output performances. Films layered with parylene derivatives, including fluorine, hydroxyl, and methyl-hydroxyl groups, exhibit negative triboelectric properties, whereas those coated with parylene incorporating the methyl-amine group exhibit positive triboelectric properties. Notably, all bilayer films layered with parylene derivatives show a dramatic increase in triboelectric output performance, which is attributed to the enhanced interfacial polarization arising from the permittivity and conductivity differences between MWCNT-PDMS and parylene derivatives. Furthermore, when bilayer films layered with parylene derivatives containing hydroxyl and methyl-amine groups serve as negative and positive triboelectric materials, respectively, in the periodic triboelectric process, we observe an even substantial enhancement in output performance ($4.57 \text{ W}/\text{cm}^2$ and $10.28 \text{ W}/\text{cm}^2$ for contact and separation steps, respectively). This result surpasses the performance of conventional PDMS-based TENGs, which typically produce less than a few of mW/cm^2 .

2. Results and discussion

Initially, we investigated the output performances of TENGs consisting of bilayer-structured films as negative triboelectric layers. The bilayer films are fabricated by depositing parylene derivatives onto the surface of MWCNT-PDMS films. Here, PLL film is employed as a positive triboelectric material (Fig. 1a). Upon contact between triboelectric pair materials (Fig. 1b-i), surface charges are generated through contact electrification, resulting in the accumulation of negative charges on the surface of parylene-deposited layer and positive charges on the surface of PLL layer. This phenomenon manifests as a negative peak (1) in

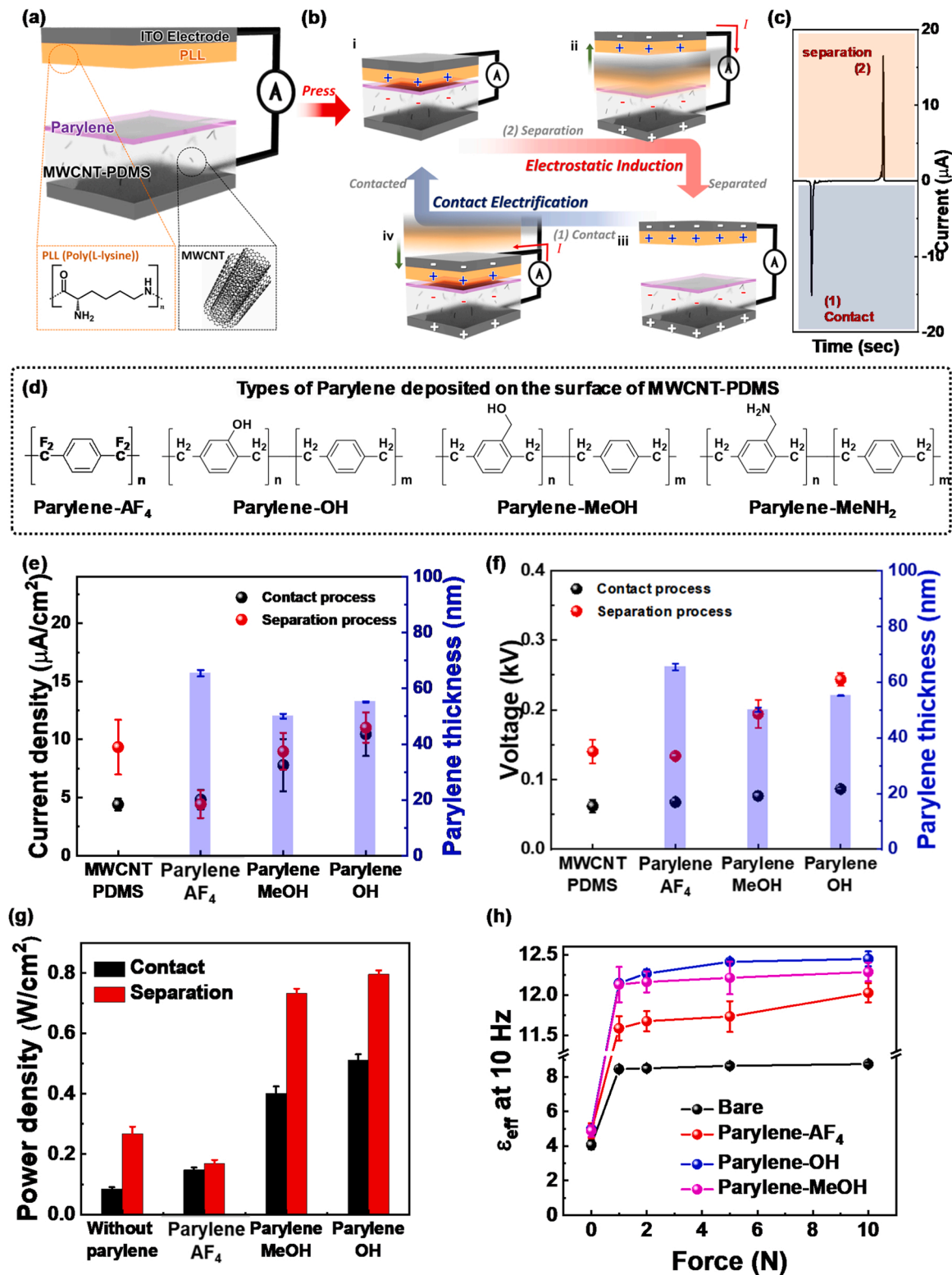


Fig. 1. (a) Schematic illustration of a triboelectric nanogenerator consisting of parylene-deposited MWCNT-PDMS and poly (L-lysine) as negative and positive triboelectric layers, respectively, and (b) its working mechanism. The cyclic contact (iv and i) and separation (ii and iii) of contact-pair materials induces charge separation and transfer, thus resulting in the current flow through the external circuit. (c) Representative triboelectric output current density of a bilayer film deposited with the optimized parylene-OH. Peaks (1) and (2) appear when both of the surfaces are contacted and separated, respectively. (d) Chemical structures of parylenes with different functional groups used in this study. Triboelectric output (e) current and (f) voltage of TENGs consisting of parylene-deposited MWCNT-PDMS and poly (L-lysine). (g) Histogram of power density of the single MWCNT-PDMS without parylene derivatives and parylene-deposited bilayer films at 20 M Ω . (h) Effective dielectric constant of MWCNT-PDMS with and without parylene derivatives at 10 Hz under different loading force. The parylene-deposited MWCNT-PDMS films are annealed at 150 °C.

Fig. 1c. As the contact pairs start to separate (Fig. 1b-ii), electrostatic induction causes opposite charges to be transferred to each electrode, leading to flow of current from positive to negative electrode through the external circuit. This results in a positive peak (2) in Fig. 1c. Once the films are fully separated, charge equilibrium is achieved on both sides of the electrodes (Fig. 1b-iii). As the films begin to approach each other again (Fig. 1b-iv), the current reverses direction, flowing from negative to positive electrodes. Consequently, the cyclic process of contact and separation between the paired films causes the alternating output performance.

To achieve highly-enhanced triboelectric performances with bilayer-structured films consisting of parylene derivatives and MWCNT-PDMS composites, we initially optimized the output performance of single-layered MWCNT-PDMS films (serving as a negative triboelectric layer) by adjusting their MWCNT concentration and thickness (Fig. S1a-d). Without MWCNT, bare PDMS displayed triboelectric currents of $2.3 \pm 0.4 \mu\text{A}$ and $8.5 \pm 2.6 \mu\text{A}$ during contact and separation, respectively. The separation triboelectric current was higher than during contact, due to the increased separation velocity resulting from enhanced surface adhesion after the conformal contact between soft PDMS and PLL films. When the MWCNT concentration was increased to 0.2 wt% relative to PDMS oligomers, the triboelectric performances improved to 4.4 ± 0.5 and $9.3 \pm 2.4 \mu\text{A}$ for contact and separation step, respectively, (Fig. S1e), due to enhanced polarization between MWCNT and PDMS [37,38]. However, further increasing the MWCNT concentration to 0.7 wt% led to a decrease in triboelectric performance, dropping to 2.6 ± 0.3 and $8.5 \pm 2.0 \mu\text{A}$ for the contact and separation step, respectively, due to the current leakage resulting from the formation of a conductive MWCNT network [37]. This trend aligns with previous reports on TENGs composed of MWCNT-PDMS [37]. Furthermore, when the optimized MWCNT-PDMS composite had a thickness of $16.0 \pm 0.1 \mu\text{m}$, it exhibited higher output performance compared to other compositions (Fig. S1b and e). This is attributed to effective charge polarization and induction to the electrode at the optimal thickness [19,20]. Ultimately, a single-layered MWCNT-PDMS with an MWCNT concentration of 0.2 wt % and a thickness of $16.0 \mu\text{m}$ was determined as the optimal condition for achieving the highest triboelectric performance in our study.

To further increase the triboelectric performances, we designed bilayer-structured films because the layered films with differences in permittivity and conductivity can induce interfacial polarization at the interfaces, which in turn enhances the effective dielectric constant and subsequently the triboelectric performance [12,20]. Given that parylene derivatives possess a different dielectric constant compared to the MWCNT-PDMS composite (Fig. S1f), depositing parylene on the surface of MWCNT-PDMS results in interfacial polarization between the parylene derivatives and the MWCNT-PDMS composite films. Since the introduction of functional groups into parylenes can modulate the polarizability of the polymer chains, we employed various parylene derivatives with different functional groups (parylene-AF₄, parylene-OH, parylene-MeOH, and parylene-MeNH₂ with fluorine, hydroxyl, methyl-hydroxyl, and methyl-amine groups, respectively, Fig. 1d and S2–S6) and deposited them onto the surface of MWCNT-PDMS (Fig. S7 and S8) to fabricate soft bilayer films. These bilayer films, consisting of parylene derivatives and MWCNT-PDMS, exhibit superior triboelectric output performances compared to the single-layer MWCNT-PDMS film (Fig. 1e and f). The separation output performances are higher than the contact ones, which is caused by higher separation velocity than the contact velocity as mentioned in Fig. S1. Notably, among these bilayer films, the one coated with parylene-OH demonstrates the best triboelectric performances (0.51 and 0.80 W/cm^2 for the contact and separation step, respectively, Fig. 1g and S9).

Triboelectric performances are mainly affected by the amounts of surface charges, which are in turn associated with factors such as surface potential, surface roughness, and dielectric constant [12,15,39]. An increased difference in surface potentials between triboelectric pair

materials can lead to an enhanced generation of surface charges through contact electrification. The tribopositive PLL film, known to exhibit a positive surface potential ($+0.85 \text{ V}$) [40] owing to the presence of electron-donating amine groups in the polymer chain, contrasts with the single-layer MWCNT-PDMS film having a surface potential of $-5.8 \pm 0.1 \text{ V}$. After parylene deposition, bilayer films show higher surface potentials ($-5.3 \pm 0.1 \text{ V}$, $-5.6 \pm 0.1 \text{ V}$, and $-5.6 \pm 0.1 \text{ V}$ after the deposition of parylene-AF₄, parylene-OH, and parylene-MeOH, respectively, Fig. S10), yet still maintain negative triboelectric properties. Although an increase in surface potential of bilayer films might typically suppress the triboelectric performance, in our study, the parylene-deposited bilayer films displayed higher triboelectric performances than the single-layer MWCNT-PDMS film. This was observed even though the surface roughness of bilayer films, a contributing factor to improved surface charge density by increasing the contact area of triboelectric-pair materials, was similar to that of single MWCNT-PDMS composite (Fig. S10). This suggests that in our study, surface potential is not a critical factor for enhancing the triboelectric performances of bilayer structured films.

Another key factor for achieving high-output performance in the triboelectric device is the dielectric constant. An increase in this constant can enhance the capacitance of the dielectric layer, leading to an improvement in surface charge density. As illustrated in Scheme S1a, in a dielectric-to-dielectric contact mode triboelectric device, it is evident that the capacitance (C) increases when the dielectric constant rises or the thickness of the dielectric layer decreases. Consequently, according to the equations in Scheme S1a, the surface charge density is directly proportional to the ratio of the dielectric constant to thickness (ϵ/d). Specifically, interfacial polarization occurs at low frequency as part of triboelectric process when space charges (electrons or ions) accumulate at the interface between two dissimilar materials that significantly differ in permittivity and electrical conductivity when subjected to an external electric field, as illustrated in Scheme S1b. The improved polarization leads to an increase in the dielectric constant and, consequently, capacitance, which enhances the surface charge and, in turn, improves the triboelectric performance. In our study, we investigated the dielectric properties of the parylene-deposited bilayer films, a significant element contributing to the enhancement of the output performances [12,20,21]. Notably, these parylene-deposited bilayer films initially display a higher effective dielectric constant compared to the single-layered MWCNT-PDMS (Fig. 1h), which is caused by the increased polarization at the interface between parylene derivatives and MWCNT-PDMS through the difference in permittivity of each film (Fig. S1f). The effective dielectric constants are further enhanced under an external loading force, leading to the highly increased capacitance and subsequent improvement of the triboelectric performance. Especially, the bilayer film deposited with parylene-OH shows the highest dielectric constant, which matches well with the trend of triboelectric performances (Fig. 1e–f).

In films with a stacked-layer structure, the thickness of the film plays a pivotal role in effectively inducing interfacial polarization, which in turn significantly affects the triboelectric performances [12,20,21]. In a thicker dielectric film, charges are less polarized under an external field, leading to the suppression of dielectric constant in the layered materials, which subsequently decrease the surface charge density and thus the resulting triboelectric performance. On the other hand, in a thinner dielectric film, the polarized charges are able to move along the electrode, leading to the current leakage (charge loss), which also decreases the surface charge density. Consequently, there exists an optimal thickness for the dielectric film that maximizes the induction of interfacial polarization. In our study, we manipulated the thickness of the parylene films deposited on the surface of MWCNT-PDMS by precisely adjusting the quantities of parylene monomers with different functional groups during the CVD deposition process. In TENGs composed of parylene-deposited bilayer films as the negative triboelectric layers and PLL as the positive triboelectric layers (Fig. 2a–c), those with the optimal

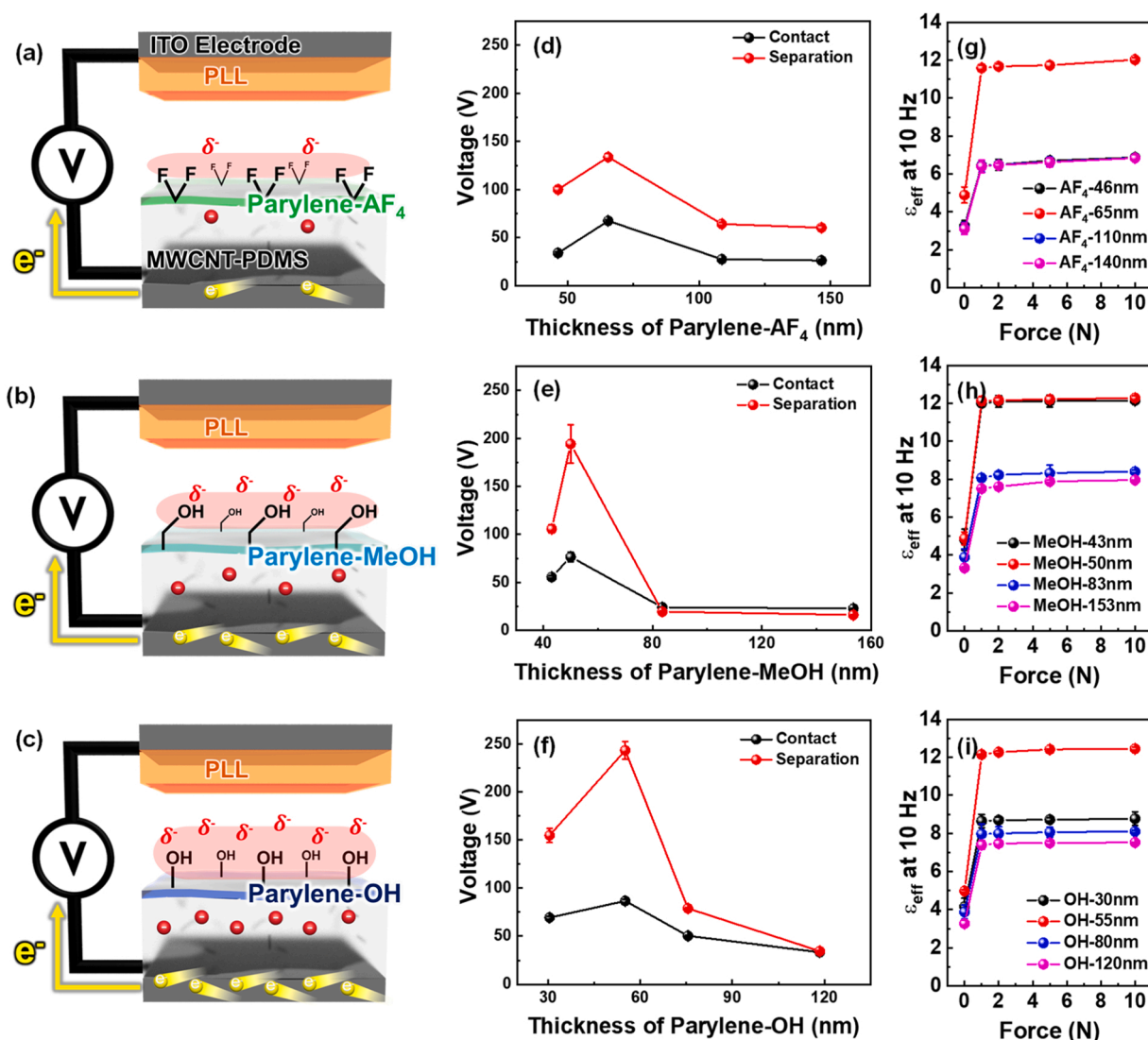


Fig. 2. (a-c) Scheme of TENGs consisting of MWCNT-PDMS with different kinds of parylenes and poly (L-lysine) as negative and positive triboelectric layers, respectively, (d-f) the triboelectric output voltages, and (g-i) the effective dielectric constant at 10 Hz under different loading force: (a, d, g) for parylene-AF₄ with different deposition thickness, (b, e, h) for parylene-MeOH with different deposition thickness, and (c, f, i) for parylene-OH with different deposition thickness. The parylene-deposited MWCNT-PDMS films are annealed at 150 °C.

parylene thickness demonstrated superior output performances compared to the others (Fig. 2d-f and S11). It should be noted that the parylene deposition thickness was measured by AFM after scratching Si substrates deposited with parylene derivatives (Fig. S11). Specifically, by optimizing the deposition thickness to 65 nm, 50 nm, and 55 nm for Parylene-AF₄, Parylene-MeOH, and Parylene-OH, respectively, we achieved triboelectric performances of 67.5 ± 1.3 V, 76.5 ± 5.0 V, and 86.7 ± 2.0 V during the contact process. During the separation process, we observed a similar pattern, where we achieved the highest output voltages of 133.9 ± 3.7 V, 194.2 ± 19.8 V, and 243.5 ± 9.2 V at the optimized thicknesses of 65 nm, 50 nm, and 55 nm for the parylene-AF₄, parylene-MeOH, and parylene-OH, respectively (Fig. 2d-f). Among the optimized parylene-bilayer films, the film deposited with parylene-OH shows the best triboelectric voltage. This result can be attributed to higher effective dielectric constant of the parylene-OH deposited bilayer film, resulting in improved interfacial polarization compared to the other films (Figs. 2g-i). It is worth noting that the bilayer films exhibit similar surface potentials and roughness (Fig. S10), suggesting minimal differences in the triboelectric performance due to their comparable triboelectric polarity and contact area. However, thanks to the increased dielectric constant through remarkable improvement of interfacial

polarization, the parylene-OH/MWCNT-PDMS bilayer film displays a higher power density (0.51 and 0.80 W/cm² for the contact and separation step, respectively) than the other bilayer films (Fig. 1g), which is the best triboelectric performance compared to the parylene-based TENGs (less than tens of μW/cm², Table S1).

Interfacial polarization, which is induced at the interfaces of dissimilar layers, is greatly affected by the interfacial properties of a layered film. In particular, the adhesion between each layer plays a pivotal role in significantly enhancing interfacial polarization. The process of parylene coating is generally divided into three main steps: sublimation, decomposition, and deposition. Of these steps, the deposition critically affects the adhesion between parylene and the target surface. The deposition of parylene on the target surface is facilitated by a free radical addition reaction of parylene derivative monomers [41, 42]. To enhance the adhesion between parylene and the surface, a silane material with a methacryloxy tail is typically utilized for the modification of the target surface, leading to covalent chemical bonding through co-polymerization between parylene monomers and the methacryloxy units [43,44]. In our research, we deposited parylene monomers with different functional groups on the surface of MWCNT-PDMS films (Fig. 3a). Before the deposition process, to improve the adhesion

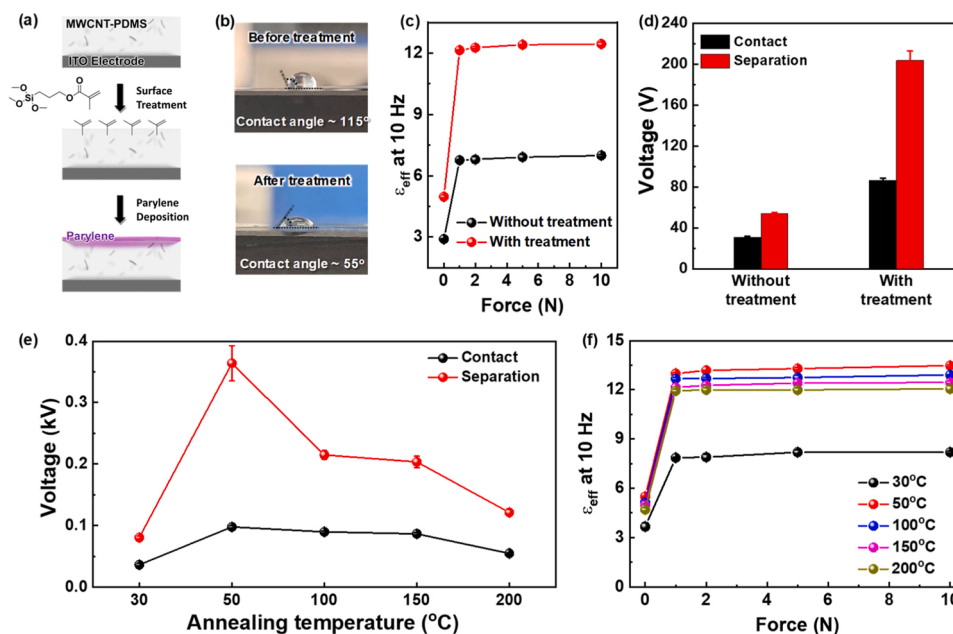


Fig. 3. Triboelectric output performances of bilayer films consisting of parylene and MWCNT-PDMS layers. (a) scheme to modify the surface of MWCNT-PDMS with 3-(Trimethoxysilyl)propyl methacrylate and then deposit the parylene-derivatives. (b) Contact angles of MWCNT-PDMS before and after the surface modification. (c) Effective dielectric constant and (d) triboelectric output voltage of parylene-OH deposited MWCNT-PDMS without and with surface treatment, respectively. The bilayer films are annealed at 150 °C. (e) Triboelectric output voltage and (f) effective dielectric constant of parylene-OH deposited MWCNT-PDMS with surface treatment, respectively. The bilayer films with constant thickness of 55 nm are annealed at different temperature from 30 to 200 °C.

between parylene and MWCNT-PDMS, 3-(trimethoxysilyl)propyl methacrylate (TPM) was initially coated on the MWCNT-PDMS surface following an oxygen plasma treatment. This treatment led to the silanization of TPM with the hydroxyl group on the MWCNT-PDMS surface. Subsequently, following the CVD process of parylene monomers, we obtained bilayer films composed of parylene and MWCNT-PDMS through copolymerization of parylene monomers with the methacryloxy units on the MWCNT-PDMS surface. The change in surface property of MWCNT-PDMS following parylene deposition was verified by measuring the contact angle (Fig. 3b). The treatment of methacryloxy units reduced the contact angle due to the increase in the surface free energy of MWCNT-PDMS. In addition, the bilayer film deposited with parylene-OH after the surface treatment exhibited a higher effective dielectric constant (12.4 ± 0.1 under 10 N) than one without the treatment (7.0 ± 0.1 under 10 N, Fig. 3c). This enhanced dielectric constant is caused by the increased interfacial polarization resulting from the conformal deposition of parylene-OH on the MWCNT-PDMS surface. It is worth noting that the parylene-OH coated bilayer film without surface treatment showed a lower dielectric constant (7.0 ± 0.1 under 10 N) even than the single-layer MWCNT-PDMS film (8.7 ± 0.1 at 10 Hz under 10 N, Fig. 1h). This result indicates that conformal deposition is vital for effective induction of interfacial polarization, which in turn affects the resulting dielectric constant. Ultimately, the bilayer film with the conformal deposition of parylene-OH effectively induces the interfacial polarization, resulting in the improvement of dielectric constant (12.4 ± 0.1 under 10 N) and thus the resultant triboelectric performance (86.7 ± 2.0 V and 203.5 ± 9.2 V for the contact and separation step, respectively, Fig. 3d and S12).

Besides the conformal deposition at the interface, the annealing process also significantly influences the triboelectric performance because of varying dielectric properties resulting from the polymer chain rearrangement [40]. We further investigated the annealing effect of the parylene-OH deposited bilayer film on the triboelectric performance. Ultimately, when the parylene-OH, with an optimized thickness of ~55 nm, is annealed at 50 °C, the bilayer film shows the best output performance (97.9 ± 2.2 V and 364.1 ± 28.8 V for the contact and

separation step, respectively, Fig. 3e and S13-S14). This is attributed to the enhanced dielectric properties (13.5 ± 0.1 under 10 N, Fig. 3f and S14), resulting from the polymer chain arrangement at the optimal film thickness.

It can be concluded that parylene derivatives with different types of functional groups that possess electron-withdrawing abilities can be utilized as a negative triboelectric layer. Stacking these materials on dielectric materials with a large permittivity difference can lead to significantly improved interfacial polarization, which affects both the dielectric constant and triboelectric output performance. In this study, while the bilayer films with parylene derivatives, including functional units such as fluorine, methyl hydroxyl, and hydroxyl groups, exhibit similar surface potentials (Fig. S10), the parylene-OH deposited bilayer film shows the best triboelectric performance because of the increased dielectric constant through the enhanced interfacial polarization.

The integration of functional groups with different electron-affinity properties into parylene-derivatives significantly affects the triboelectric polarities of parylene-deposited bilayer films, thereby altering their triboelectric performance. Specifically, parylene-derivatives incorporating electron-withdrawing units, such as fluorine, methyl-hydroxyl, and hydroxyl, displayed a negative triboelectric property, which enhanced the output performances of bilayer films compared to the single layer film. It implies that the functional groups incorporated into the parylene-derivatives are another key factor in boosting the triboelectric performances. In contrast to using electron-withdrawing units, we incorporated a methyl amine group with the electron-donating ability into the parylene monomer and investigated its surface and triboelectric properties. Interestingly, the bilayer film deposited with parylene-MeNH₂ displays a positive surface potential (+1.29 V, Fig. S15a), which is higher than that of the PLL layer (+0.85 V). Moreover, the bilayer film deposited with electron-donating parylene-MeNH₂ displays an opposite polarity of triboelectric signals to those deposited with parylene derivatives containing electron-withdrawing units. During the cyclic triboelectric process involving the bilayer film and PLL (Fig. 4a), alternating current signals are observed: peak (1) presents a positive current signal, and peak (2) a negative current signal,

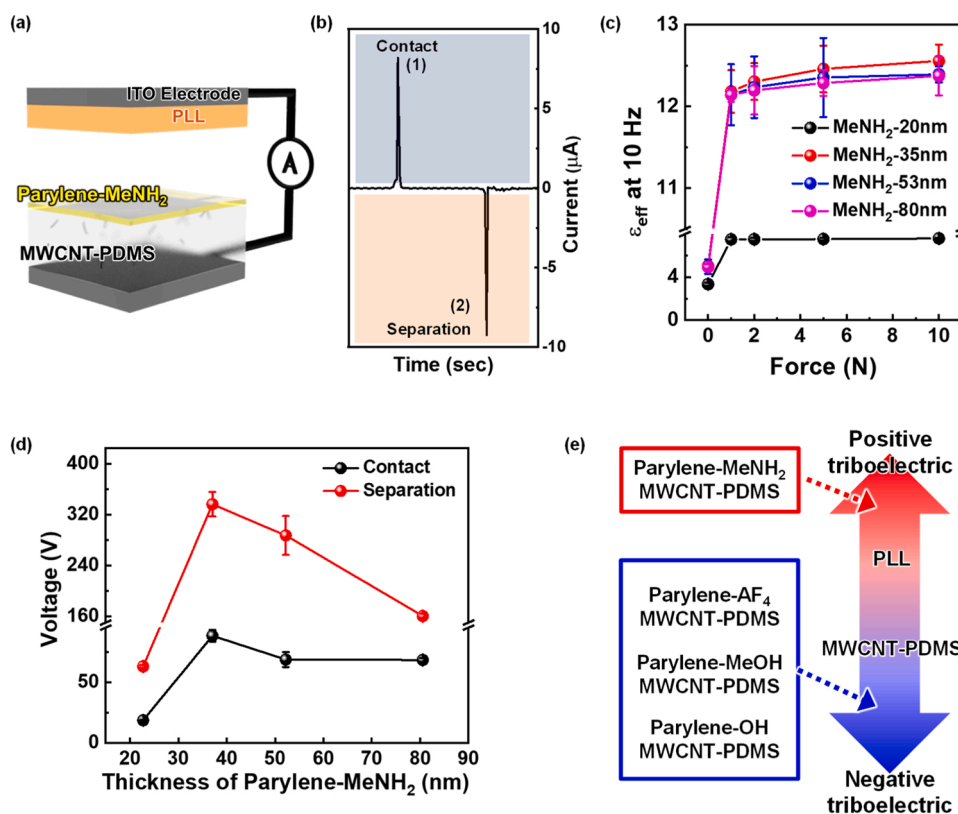


Fig. 4. (a) Scheme of a triboelectric device consisting of MWCNT-PDMS deposited with the optimized parylene-MeNH₂. (b) Representative triboelectric output current. Peaks (1) and (2) appear when both of the surfaces are contacted and separated, respectively. (c) Effective dielectric constant and (d) output voltage of the MWCNT-PDMS deposited with parylene-MeNH₂ with different thickness. (e) Triboelectric series of bilayer films consisting of MWCNT-PDMS deposited with different kinds of parylene-derivatives. The parylene-deposited MWCNT-PDMS films are annealed at 150 °C.

corresponding to the contact and separation processes, respectively (Fig. 4b). This signal generation pattern is opposite to those with electron-withdrawing parylene derivatives (Fig. 1c). It indicates that the introduction of MeNH₂ units with electron-donating properties into the parylene monomer affects the surface potential, resulting in a higher positive potential (+1.29 V) than PLL (+0.85 V). Additionally, we examined the dielectric properties of parylene-MeNH₂ deposited bilayer films with different thicknesses (Fig. 4c and S15). When the deposition thickness of parylene-MeNH₂ is 35 nm, the bilayer film shows the highest effective dielectric constant (12.6 ± 0.2 at 10 Hz under 10 N), leading to the best triboelectric output performances (88.2 ± 4.8 V and 336.4 ± 19.3 V for the contact and separation step, respectively, Fig. 4d and S15b). However, this output performance is still lower than that of the optimized parylene-OH/MWCNT-PDMS bilayer film (Fig. S16).

The deposition of parylene derivatives with diverse functional groups onto the surface of MWCNT-PDMS affects both surface and dielectric properties, resulting in the enhancement of triboelectric performances. The bilayer films deposited with parylene derivatives containing electron withdrawing units exhibit similar negative surface potentials. However, these films possess unique dielectric properties (Fig. S1f) due to varying interfacial polarization resulting from the distinct contrast of permittivity between parylene derivatives and MWCNT-PDMS, significantly influencing the triboelectric performances. Based on these results, the bilayer films can be ordered in terms of negative triboelectric series as follows: parylene-OH/MWCNT-PDMS > parylene-MeOH/MWCNT-PDMS > parylene-AF₄/MWCNT-PDMS > MWCNT-PDMS. On the other hand, the bilayer film deposited with parylene derivatives containing electron donating units (MeNH₂) displays a positive surface potential. This positive bilayer film exhibits an increased dielectric constant through the improved interfacial polarization, compared to the other parylene-derivatives used in this study,

resulting in a superior triboelectric performance than the PLL positive triboelectric layer. In terms of output performance, the bilayer films are ranked as follows: parylene-OH/MWCNT-PDMS > parylene-MeNH₂/MWCNT-PDMS > parylene-MeOH/MWCNT-PDMS > parylene-AF₄/MWCNT-PDMS > MWCNT-PDMS. These results suggest that the bilayer film can serve as an attractive triboelectric material, significantly enhancing the triboelectric performance.

Considering the dielectric properties and triboelectric series, we designed bilayer films utilizing optimized parylene-OH and parylene-MeNH₂ as negative and positive triboelectric materials, respectively, which can further enhance the triboelectric performance. The large difference in surface potential between each bilayer film allows for the generation of more charges upon contact compared to using a single PLL layer as a positive triboelectric material. Moreover, the higher dielectric constants of bilayer films compared to the single layer ones enables a greater production of charges on the surface of bilayer-pair materials. These charges are then transferred to the electrode, resulting in a substantial increase in output performances: 17.8 ± 2.6 μ A and 111.1 ± 4.4 V for the contact step and 37.1 ± 2.9 μ A and 443.6 ± 14.0 V for the separation step (Fig. 5a-b). Especially, the optimized parylene-OH/MWCNT-PDMS bilayer film, serving as a negative triboelectric layer, when combined with the optimized parylene-MeNH₂/MWCNT-PDMS as a positive triboelectric layer, results in a power density (4.57 W/cm² and 10.28 W/cm² for contact and separation step, respectively) that is more than 10 times greater than that (0.51 W/cm² and 0.80 W/cm² for contact and separation step, respectively) of the PLL layer in the triboelectric performance (Fig. S16 and S17). These bilayer-pair films show the best triboelectric performance (more than a few of W/cm²) compared to other parylene- or PDMS-based TENGs (less than a few of mW/cm², Table S1 and S2). Moreover, the triboelectric device consisting of parylene-OH and parylene-MeNH₂ deposited bilayer films,

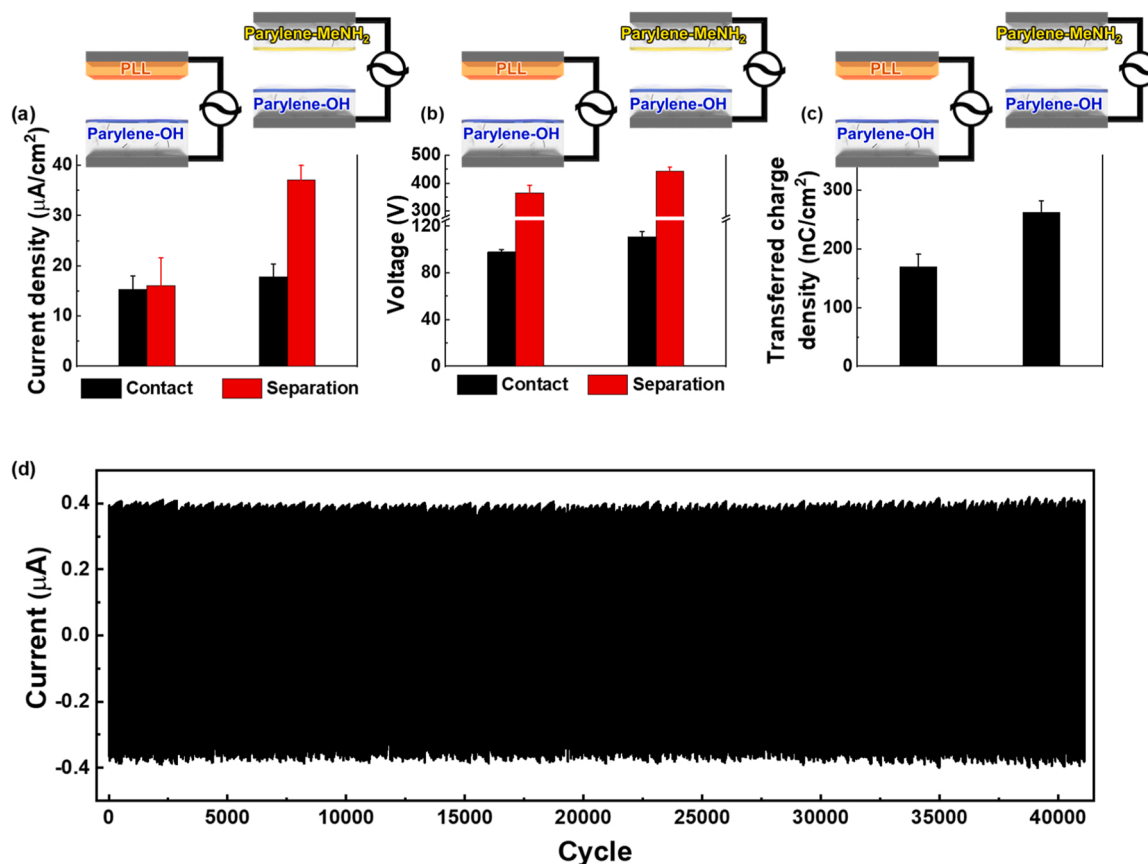


Fig. 5. Triboelectric output performances of contact-pair materials including single-bilayer (PLL/parylene-OH deposited MWCNT-PDMS) films, and bilayer-bilayer (parylene-MeNH₂ deposited MWCNT-PDMS/parylene-OH deposited MWCNT-PDMS) films, respectively: (a) output current density, (b) output voltage, and (c) transferred charge density. The bilayer films are annealed at 50 °C for parylene-OH deposited film and 150 °C for parylene-MeNH₂ film. (d) Stability of triboelectric device consisting of bilayer-pair films deposited with the optimized parylene-OH and parylene-MeNH₂ as negative and positive triboelectric layers, respectively, at 2 N over 40000 cycles.

serving as negative and positive triboelectric materials, respectively, exhibits stability over 40000 cycles.

In our study, we designed bilayer-structured films composed of MWCNT-PDMS and parylene derivatives. These films induce significant interfacial polarization due to a substantial contrast in permittivity and conductivity between the dielectric layer films, resulting in a considerable increase in the dielectric constant and, consequently, enhanced triboelectric performance. Furthermore, the type of functional groups present in the parylene derivatives determines the bilayer films' triboelectric polarity. Bilayer films with parylene derivatives containing electron-withdrawing groups such as fluorine, methyl-hydroxyl, and hydroxyl units exhibit negative triboelectric properties (Fig. S10), whereas those with parylene derivatives containing electron-donating groups like the methyl-amine unit display positive triboelectric behavior (Fig. S15). These findings suggest that the bilayer film can serve as an appealing triboelectric material, significantly augmenting triboelectric performance. Specifically, the bilayer films deposited with optimized parylene-OH and parylene-MeNH₂ exhibited the best triboelectric performances among the negative and positive triboelectric materials, respectively (Fig. S9 and S16), which is attributed to the significant enhancement of the dielectric constant resulting from highly induced interfacial polarization. Building upon the enhanced dielectric and triboelectric performances of the optimized negative and positive triboelectric layers, we designed bilayer-pair films to further boost the output performance. These bilayer-pair films, composed of parylene-OH (negative) and parylene-MeNH₂ (positive) deposited on MWCNT-PDMS, demonstrated superior triboelectric performance (Fig. 5 and S17) thanks to their negative and positive triboelectric polarities, coupled with the

significantly increased dielectric constant.

3. Conclusion

In this study, we demonstrated a high-performance TENG based on a simple structure consisting of parylene derivatives and MWCNT-PDMS films. The parylene derivatives with different kinds of functional groups were deposited at nanometer scale on the surface of MWCNT-PDMS films, producing the bilayer structured films. The bilayered film resulted in the improved interfacial polarization, leading to the enhanced triboelectric performances, which is significantly higher than the single layer film. Furthermore, we investigated factors such as the kinds of functional groups in the parylene derivatives, deposition thickness, and annealing temperature in order to effectively induce the interfacial polarization. Consequently, as the parylene-OH with the thickness of ~55 nm annealed at 50 °C is deposited on the MWCNT-PDMS surface, the bilayer film shows the best triboelectric performance compared to the parylene-based TENGs. On the other hand, the functional groups introduced in the parylene derivatives affected the triboelectric properties of bilayer films. When the electron withdrawing units such as fluorine, methyl-hydroxyl, and hydroxyl groups were introduced in the parylene derivatives, the bilayer films displayed the output performances of negative triboelectric materials. On the other hand, the bilayer film deposited with parylene including the electron donating unit (methyl-amine group) showed the output performances of a positive triboelectric material. Moreover, the contact-pairs consisting of bilayer films as negative and positive triboelectric materials showed significant enhancement of triboelectric performance (4.57 W/cm² and

10.28 W/cm² for the contact and separation steps, respectively), which is the best output performance compared to those conventional ones based on PDMS or parylene layers (less than a few mW/cm²). These findings suggest that layer-structured films with pronounced differences in permittivity and conductivity hold promise as candidates for triboelectric materials, capable of dramatically improving output performance. Furthermore, beyond layer-stacking structures, the introduction of thin derivatives with distinct functional groups onto the same polymers enables the creation of distinct triboelectric polarities and even more substantial enhancements in triboelectric performance through improved polarization. This approach offers a straightforward yet effective method for designing self-powered flexible devices with high-output performance.

4. Experimental

4.1. Materials

The commercial dimer used for the Parylene CVD was purchased from YSMTTC (Taiwan); Octafluoro[2.2]paracyclophane (Parylene-AF₄) ($\geq 99.0\%$). As the reagents for synthesizing the dimer, [2.2]paracyclophane ($\geq 99.0\%$) (NURI TECH. CO., Republic of Korea) titanium (IV) chloride (ReagentPlus, 99.9%, Sigma Aldrich, USA), 1,1-dichlorodimethyl ether (97%, ACROS, USA), hydrogen peroxide (35% in water, TCI, Japan), sodium borohydride (granular, 99.99%, Sigma Aldrich, USA), phosphorus tribromide (99%, Sigma Aldrich, USA), phthalimide potassium salt (98%, Sigma Aldrich, USA), hydrazine hydrate (50–60%, Sigma Aldrich, USA) were used without purification. Sodium sulfate (98.5%), sodium bicarbonate (99.0–100.5%), sodium chloride (99.0%), sulfuric acid (95.0%), hydrochloric acid (3 N), dichloromethane (99.8%), methyl alcohol (99.8%), n-hexane (99.5%), ethyl acetate (99.5%), tetrahydrofuran (Stabilized, 99.8%), N,N-dimethylformamide (99.5%) were purchased from SAMCHUN CHEMICALS (Republic of Korea).

Fourier Transform- Infrared Spectroscopy (FT-IR, Spectrum Two, Perkinelmer, Republic of Korea), Field Emission Scanning Electron Microscope (FE-SEM, CLARA, TESCAN, Czech Republic), Custom-made CVD Polymerization equipment (TeraLeader, Republic of Korea), Hot presser (Qmesys, Republic of Korea).

4.2. Synthesis of parylene derivatives

4.2.1. Synthesis of 4-hydroxyl[2.2]paracyclophane

[2.2]Paracyclophane (3 g, 14.3 mmol) were immersed in 200 mL of dichloromethane in round bottom flask (RB) at 0 °C with N₂ inert atmosphere. After TiCl₄ (3.15 mL, 21.7 mmol) was added dropwise, the mixture was stirred for 1 h. And then, 1, 1-dichlorodimethyl ether (1.33 mL, 15 mmol) was injected dropwise. After stirring for 1.5 h, the reaction was quenched by water. The crude solution was washed by HCl (3 N) and sodium bicarbonate solution, and sodium sulfate. Through column chromatography using n-hexane: ethyl acetate = 40:1 solution, the 4-formyl[2.2]paracyclophane could be obtained with colorless white powder (3.04 g, 90%). 4-Formyl[2.2]paracyclophane (3.00 g, 12.7 mmol) were dissolved in dichloromethane (60 mL) and methyl alcohol (60 mL). Put the sulfuric acid (0.096 mL) and hydrogen peroxide (1.44 mL, 35% in water) in order and the solution was stirred for 16 h at RT. After removing the solvent by rotary evaporator, the solid residue was washed with dichloromethane and water. Finally, the yellowish powder (2.69 g, 95.2%) could be obtained by column chromatography (n-hexane:ethyl acetate = 25:1).

4.2.2. Synthesis of 4-hydroxymethyl[2.2]paracyclophane

4-Formyl[2.2]paracyclophane (3 g, 12.7 mmol) was dissolved in methyl alcohol (200 mL) and tetrahydrofuran (10 mL). Then sodium borohydride (1 g, 26.4 mmol) was added carefully and it was stirred for 3 h. After the solvent was removed by the rotary evaporator, the product

should be washed with hydrochloric acid (3 N) and water dissolved in dichloromethane. White powder of 4-hydroxymethyl[2.2]paracyclophane (2.77 g, 11.6 mmol) was gathered by column chromatography.

4.2.3. Synthesis of 4-aminomethyl[2.2]paracyclophane

4-Hydroxymethyl[2.2]paracyclophane (3 g, 12.6 mmol) was dissolved in dichloromethane (150 mL) at 0 °C in N₂ atmosphere. Phosphorus tribromide (1.5 mL, 5.5 mmol) was added dropwise and the reagents were reacted for 4 h. The mixture was hydrolyzed by water and washed with hydrochloric acid (3 N), sodium bicarbonate solution, and sodium chloride solution. Removing the solvent, 4-bromomethyl[2.2]paracyclophane was obtained. 4-Bromomethyl[2.2]paracyclophane (3 g, 9.9 mmol) and potassium phthalimide (1.92 g, 10.4 mmol) were dissolved together in N,N-dimethylformamide (100 mL). These reactants were heated at 80 °C for 4 h and washed sodium chloride solution, dichloromethane, and sodium sulfate. The product obtained (3 g) was immersed in methyl alcohol (300 mL) and injected hydrazine hydrate (4.58 g, 42.9 mmol). After removing the solvent, the crude product was taken the co-solvent of dichloromethane (250 mL) and 1 M sodium hydroxide solution (300 mL). The phase-separated solution was washed with dichloromethane, sodium sulfate, 1 M sodium hydroxide solution, and sodium chloride solution. The purified product, 4-aminomethyl[2.2]paracyclophane (1.09 g, 23.8%), was obtained by the column chromatography.

4.3. Parylene deposition by CVD method

Before Parylene deposition, the surface of MWCNT-PDMS is treated by silane materials including methacryloxy units according to the reported procedure [51]. Briefly, 1 mL of 3-(trimethoxysilyl) propyl methacrylate (TPM) is added into the solution consisting of 100 mL of isopropyl alcohol and 100 mL of deionized water. After the mixture is stirred for 150 min, the MWCNT-PDMS treated by oxygen plasma is put into the mixture over 120 min. The samples are rinsed with isopropyl alcohol to remove the unreacted TPMs and then, dried at 120 °C for 30 min. Afterward, four kinds of parylene derivatives are deposited via CVD by Gorham method using Custom-made CVD Polymerization equipment (TeraLeader, Republic of Korea). Octafluoro[2.2]paracyclophane (90 mg) are used for depositing Parylene-AF₄ about 65 nm thickness. Once this dimer is sublimated from solid powder to vapor phase, it moves to pyrolysis zone (760 ~ 770 °C) along the inert Argon carrier gas (20 sccm). In the pyrolysis zone, the dimer can be cleaved to monomers in radical form, which are participated in polymerization on the surface of MWCNT-PDMS. The samples are put on the rotating sample holder cooled down to - 5 °C in the heating chamber (60 °C). Besides, 4-hydroxyl, 4-hydroxymethyl, and 4-aminomethyl [2.2] paracyclophane have same temperature conditions pyrolyzed at 550 ~ 560 °C and deposited on 5 °C holder in 80 °C heating chamber. But to deposit an optimal thickness of each parylene, different amount of dimer quantities are needed; for example, 80 mg of 4-hydroxyl[2.2]paracyclophane for 55 nm of parylene-OH, 20 mg of 4-hydroxymethyl[2.2]paracyclophane for 50 nm of parylene-MeOH, and 60 mg of 4-aminomethyl[2.2]paracyclophane for 35 nm of parylene-MeNH₂. Overall process is performed at a pressure level of about 150 mTorr. The deposition thickness was measured by using AFM after scratching the surface deposited with parylene derivatives on a piece of Si wafer.

4.4. Annealing treatment

After the CVD deposition, the thermal treatment is performed at 150 °C for 2 h to improve the adhesion properties of PDMS and parylene and to maximize the performance of triboelectric performance. In the case of parylene-OH, the optimized treatment condition is 50 °C for 2 h.

4.5. Preparation of MWCNT-PDMS composite films

In order to prepare the MWCNT-PDMS composite films, the multi-walled carbon nanotubes (MWCNT, Sigma-Aldrich, 110–190 nm diameter and 5–9 μm length) are added into the PDMS oligomer in chloroform, and then the mixture is ultrasonicated with a probe tip for 3 min, producing homogeneous dispersed MWCNT-PDMS composite. After the solvent evaporation on the hot plate, the composite mixture is combined with a curing agent (0.1 wt ratio to the PDMS oligomer). After vigorously stirring and degassing to remove the air bubble for 1 hr, the mixture is spin-coated on the surface of ITO substrate treated by oxygen plasma, followed by curing at 70 $^{\circ}\text{C}$, which produces ITO coated with the MWCNT-PDMS composite film.

4.6. Preparation of TENGs

To fabricate the triboelectric nanogenerator, 0.1 wt% of positive-charged polymer (PLL) in deionized water is spin-coated onto the ITO substrate as a positive triboelectric layer whereas MWCNT-PDMSs deposited with parylene derivatives with different kinds of functional groups are utilized as negative triboelectric layers. To further improve the triboelectric performance, the MWCNT-PDMSs deposited with parylene derivatives having electron-donor properties such as parylene-AF₄, parylene-OH, and parylene-MeOH are used as negative triboelectric layers whereas one deposited with parylene-MeNH₂ having electron-withdrawing property is used as a positive triboelectric layer.

5. Characterization

To obtain the effective dielectric constants of the polymer films, the capacitances are measured by a metal-insulator-metal capacitance method using an impedance analyzer (IM3570) at room temperature. The samples were prepared by sandwiching the dielectric films between two electrodes—an ITO electrode and a Pt electrode. Each sample is spin-coated on the cleaned ITO electrode, and then the Pt electrode (2.0 mm in diameter) is deposited on the sample surface. The effective dielectric constant is calculated as follows: $\varepsilon = (C \bullet d) / (\varepsilon_0 \bullet A)$, where C, d, A, and ε_0 denote the capacitance, film thickness, measured area, and permittivity in vacuum, respectively. We measured the capacitances of the dielectric constants of bilayer films above 10 Hz and single-layer parylene-derivative films with thicknesses below hundreds of nanometers above 1 kHz due to the surrounding noise condition. The measurements of the surface potentials are carried out using a multimode AFM (Bruker) system with Pt/Ir-coated silicon tips (tip radius 25 nm; force constant 3 N/m; resonance frequency 75 kHz). The potential difference between the AFM tip and ITO film was measured before each analysis. The performance (output current, output voltage, and transferred charge) of the triboelectric device based on the dielectric polymer film ($1 \times 1 \text{ cm}^2$) was measured using a sourcemeter (S-2400, Keithley) and an oscilloscope (DPO 2022B, Tektronix, US) under loading of 10 N by means of a pushing tester (JIPT-100, Junil Tech). The average power densities were calculated by measuring the output currents under various resistance according to the equation of $P = I^2 R$. The transferred charge densities were calculated according to the equation of $Q_{\text{SC}} = \int I_{\text{SC}} dt$.

CRediT authorship contribution statement

Minsoo P. Kim: Conceptualization, Methodology, Formal analysis, Validation. Writing - original draft. **Gunoh Lee:** Methodology, Formal analysis, Visualization. **Byeongil Noh:** Methodology, Resources. **Jaehyun Kim:** Methodology, Resources. **Min Sub Kwak:** Investigation. **Kyung Jin Lee:** Supervision, Conceptualization, Writing - review & editing. **Hyunhyub Ko:** Supervision, Conceptualization, Writing - review & editing.

Declaration of Competing Interest

The authors declare that they have no known competing financial interests or personal relationships that could have appeared to influence the work reported in this paper. Minsoo P. Kim, Ulsan National Institute of Science and Technology and Sunchon National University. Gunoh Lee, Chungnam National University. Byeongil Noh, Chungnam National University. Jaehyun Kim, Chungnam National University. Min Sub Kwak, Ulsan National Institute of Science and Technology. Kyung Jin Lee, Chungnam National University. Hyunhyub Ko, Ulsan National Institute of Science and Technology.

Data Availability

Data will be made available on request.

Acknowledgements

This work was supported by the National Research Foundation (NRF) of Korea (2021R1A2C3009222, 2022M3H4A1A02076825) and Ministry of Trade, Industry and Energy (20010566). The Commercialization Promotion Agency for R&D Outcomes (COMPA) also supported this research (MSIT: 2021-RMD-S03). This Research has also been performed as ks2322–10 KRICT core project.

Appendix A. Supporting information

Supplementary data associated with this article can be found in the online version at [doi:10.1016/j.nanoen.2023.109087](https://doi.org/10.1016/j.nanoen.2023.109087).

References

- [1] H. Fang, J. Guo, H. Wu, Wearable triboelectric devices for haptic perception and VR/AR applications, *Nano Energy* 96 (2022), 107112, <https://doi.org/10.1016/j.nanoen.2022.107112>.
- [2] J. Yin, R. Hinchet, H. Shea, C. Majidi, Wearable soft technologies for haptic sensing and feedback, *Adv. Funct. Mater.* 31 (2021), 2007428, <https://doi.org/10.1002/adfm.202007428>.
- [3] C. Xu, Y. Song, M. Han, H. Zhang, Portable and wearable self-powered systems based on emerging energy harvesting technology, *Microsyst. Nanoeng.* 7 (2021), 25, <https://doi.org/10.1038/s41378-021-00248-z>.
- [4] Y. Zhang, M. Xie, V. Adamaki, H. Khanbarez, C.R. Bowen, Control of electrochemical processes using energy harvesting materials and devices, *Chem. Soc. Rev.* 46 (2017) 7757–7786, <https://doi.org/10.1039/C7CS00387K>.
- [5] D. Choi, Y. Lee, Z.-H. Lin, S. Cho, M. Kim, C.K. Ao, S. Soh, C. Sohn, C.K. Jeong, J. Lee, M. Lee, S. Lee, J. Ryu, P. Parashar, Y. Cho, J. Ahn, I.-D. Kim, F. Jiang, P. S. Lee, G. Khandelwal, S.-J. Kim, H.S. Kim, H.-C. Song, M. Kim, J. Nah, W. Kim, H. G. Menge, Y.T. Park, W. Xu, J. Hao, H. Park, J.-H. Lee, D.-M. Lee, S.-W. Kim, J. Y. Park, H. Zhang, Y. Zi, R. Guo, J. Cheng, Z. Yang, Y. Xie, S. Lee, J. Chung, I.-K. Oh, J.-S. Kim, T. Cheng, Q. Gao, G. Cheng, G. Gu, M. Shim, J. Jung, C. Yun, C. Zhang, G. Liu, Y. Chen, S. Kim, X. Chen, J. Hu, X. Pu, Z.H. Guo, X. Wang, J. Chen, X. Xiao, X. Xie, M. Jarin, H. Zhang, Y.-C. Lai, T. He, H. Kim, I. Park, J. Ahn, N.D. Huynh, Y. Yang, Z.L. Wang, J.M. Baik, D. Choi, Recent advances in triboelectric nanogenerators: from technological progress to commercial applications, *ACS Nano* 17 (2023) 11087–11219, <https://doi.org/10.1021/acsnano.2c12458>.
- [6] J. Li, J. Cai, J. Yu, Z. Li, B. Ding, The rising of fiber constructed piezo/triboelectric nanogenerators: from material selections, fabrication techniques to emerging applications, *Adv. Funct. Mater.* (2023), 2303249, <https://doi.org/10.1002/adfm.202303249>.
- [7] M. Zhu, J. Li, J. Yu, Z. Li, B. Ding, Superstable and intrinsically self-healing fibrous membrane with bionic confined protective structure for breathable electronic skin, *Angew. Chem. Int. Ed.* 61 (2022), e202200226, <https://doi.org/10.1002/anie.202200226>.
- [8] X. Lv, Y. Liu, J. Yu, Z. Li, B. Ding, Smart fibers for self-powered electronic skins, *Adv. Fiber Mater.* 5 (2023) 401–428, <https://doi.org/10.1007/s42765-022-00236-6>.
- [9] P. Basset, S.P. Beeby, C. Bowen, Z.J. Chew, A. Delbani, R.D.I.G. Dharmasena, B. Dudem, F.R. Fan, D. Galayko, H. Guo, J. Hao, Y. Hou, C. Hu, Q. Jing, Y.H. Jung, S.K. Karan, S. Kar-Narayan, M. Kim, S.-W. Kim, Y. Kuang, K.J. Lee, J. Li, Z. Li, Y. Long, S. Priya, X. Pu, T. Ruan, S.R.P. Silva, H.S. Wang, K. Wang, X. Wang, Z. L. Wang, W. Wu, W. Xu, H. Zhang, Y. Zhang, M. Zhu, Roadmap on nanogenerators and piezotronics, *APL Mater.* 10 (2022), 109201, <https://doi.org/10.1063/5.0085850>.
- [10] H. Zou, Y. Zhang, L. Guo, P. Wang, X. He, G. Dai, H. Zheng, C. Chen, A.C. Wang, C. Xu, Quantifying the triboelectric series, *Nat. Commun.* 10 (2019), 1427, <https://doi.org/10.1038/s41467-019-09461-x>.

- [11] I. Aazem, A. Babu, S.C. Pillai, Surface patterning strategies for performance enhancement in triboelectric nanogenerators, *Results Eng.* (2022), 100756, <https://doi.org/10.1016/j.rineng.2022.100756>.
- [12] M.P. Kim, D.-S. Um, Y.-E. Shin, H. Ko, High-performance triboelectric devices via dielectric polarization: a review, *Nanoscale Res. Lett.* 16 (2021) 1–14.
- [13] J. Chen, H. Guo, X. He, G. Liu, Y. Xi, H. Shi, C. Hu, Enhancing performance of triboelectric nanogenerator by filling high dielectric nanoparticles into sponge PDMS film, *ACS Appl. Mater. Interfaces* 8 (2016) 736–744, <https://doi.org/10.1021/acsami.5b09907>.
- [14] J. Kim, H. Ryu, J.H. Lee, U. Khan, S.S. Kwak, H.J. Yoon, S.W. Kim, High permittivity CaCu₃Ti₄O₁₂ particle-induced internal polarization amplification for high performance triboelectric nanogenerators, *Adv. Energy Mater.* 10 (2020), 1903524, <https://doi.org/10.1002/aenm.201903524>.
- [15] D.W. Kim, J.H. Lee, J.K. Kim, U. Jeong, Material aspects of triboelectric energy generation and sensors, *NPG Asia Mater.* 12 (2020) 6, <https://doi.org/10.1038/s41427-019-0176-0>.
- [16] J.W. Lee, H.J. Cho, J. Chun, K.N. Kim, S. Kim, C.W. Ahn, I.W. Kim, J.-Y. Kim, S.-W. Kim, C. Yang, Robust nanogenerators based on graft copolymers via control of dielectrics for remarkable output power enhancement, *Sci. Adv.* 3 (2017), e1602902, <https://doi.org/10.1126/sciadv.1602902>.
- [17] M.P. Kim, Y.-R. Kim, H. Ko, Anisotropic silver nanowire dielectric composites for self-healable triboelectric sensors with multi-directional tactile sensitivity, *Nano Energy* 92 (2022), 106704, <https://doi.org/10.1016/j.nanoen.2021.106704>.
- [18] S. Cheon, H. Kang, H. Kim, Y. Son, J.Y. Lee, H.J. Shin, S.W. Kim, J.H. Cho, High-performance triboelectric nanogenerators based on electrospun polyvinylidene fluoride-silver nanowire composite nanofibers, *Adv. Funct. Mater.* 28 (2018), 1703778, <https://doi.org/10.1002/adfm.201703778>.
- [19] X. Chen, J.-K. Tseng, I. Treuhold, M. Mackey, D.E. Schuele, R. Li, M. Fukuto, E. Baer, L. Zhu, Enhanced dielectric properties due to space charge-induced interfacial polarization in multilayer polymer films, *J. Mater. Chem. C* 5 (2017) 10417–10426, <https://doi.org/10.1039/C7TC03653A>.
- [20] M.P. Kim, C.W. Ahn, Y. Lee, K. Kim, J. Park, H. Ko, Interfacial polarization-induced high-k polymer dielectric film for high-performance triboelectric devices, *Nano Energy* 82 (2021), 105697.
- [21] Y. Park, Y.-E. Shin, J. Park, Y. Lee, M.P. Kim, Y.-R. Kim, S. Na, S.K. Ghosh, H. Ko, Ferroelectric multilayer nanocomposites with polarization and stress concentration structures for enhanced triboelectric performances, *ACS nano* 14 (2020) 7101–7110, <https://doi.org/10.1021/acsnano.0c01865>.
- [22] T. Moss, A. Greiner, Functionalization of poly (para-xylylene) s-opportunities and challenges as coating material, *Adv. Mater. Interfaces* 7 (2020), 1901858, <https://doi.org/10.1002/admi.201901858>.
- [23] M. Golda-Cepa, K. Engvall, M. Hakkarainen, A. Kotarba, Recent progress on parylene C polymer for biomedical applications: a review, *Prog. Org. Coat.* 140 (2020), 105493, <https://doi.org/10.1016/j.porgcoat.2019.105493>.
- [24] J.J. Shao, W. Tang, T. Jiang, X.Y. Chen, L. Xu, B.D. Chen, T. Zhou, C.R. Deng, Z. L. Wang, A multi-dielectric-layered triboelectric nanogenerator as energized by corona discharge, *Nanoscale* 9 (2017) 9668–9675, <https://doi.org/10.1039/C7NR02249B>.
- [25] A.N. Ravichandran, M. Ramuz, S. Blayac, Increasing surface charge density by effective charge accumulation layer inclusion for high-performance triboelectric nanogenerators, *MRS Commun.* 9 (2019) 682–689, <https://doi.org/10.1557/mrc.2019.64>.
- [26] H. Ko, E.-H. Lee, G.-Y. Lee, J. Kim, B.-J. Jeon, M.-H. Kim, J.-C. Pyun, One step immobilization of peptides and proteins by using modified parylene with formyl groups, *Biosens. Bioelectron.* 30 (2011) 56–60, <https://doi.org/10.1016/j.bios.2011.08.026>.
- [27] E.J. Shin, W.G. Lee, S.J. Moon, Characterization of a novel antibody immobilization combining protein G with parylene-H for surface plasmon resonance immunosensors, *Microsyst. Technol.* 22 (2016) 2093–2099, <https://doi.org/10.1007/s00542-015-2534-3>.
- [28] B. Jin, G.-Y. Lee, C. Park, D. Kim, W. Choi, J.-W. Yoo, J.-C. Pyun, J.-S. Lee, Electrical characteristics and pH response of a parylene-H sensing membrane in a Si-nanonet ion-sensitive field-effect transistor, *Sensors* 18 (2018) 3892, <https://doi.org/10.3390/s18113892>.
- [29] M. Park, J. Kim, K. Kim, J.-C. Pyun, G.Y. Sung, Parylene-coated polytetrafluoroethylene-membrane-based portable urea sensor for real-time monitoring of urea in peritoneal dialysate, *Sensors* 19 (2019) 4560, <https://doi.org/10.3390/s19204560>.
- [30] M. Mariello, E. Scarpa, L. Algieri, F. Guido, V.M. Mastronardi, A. Qualtieri, M. De Vittorio, Novel flexible triboelectric nanogenerator based on metallized porous PDMS and parylene C, *Energies* 13 (2020) 1625, <https://doi.org/10.3390/en13071625>.
- [31] M. Mariello, E. Scarpa, L. Algieri, F. Guido, V. Mastronardi, A. Qualtieri, M. De Vittorio, Mechanical energy harvesting through a novel flexible contact-separation mode triboelectric nanogenerator based on metallized porous PDMS and Parylene-C, 2019 19th International Conference on Micro and Nanotechnology for Power Generation and Energy Conversion Applications (PowerMEMS), IEEE (2019) 1–4.
- [32] Y. Chiu, M. Lee, S. Wu, PDMS-based flexible energy harvester with parylene electret and copper mesh electrodes, *J. Micromech. Microeng.* 25 (2015), 104007, <https://doi.org/10.1088/0960-1317/25/10/104007>.
- [33] Y. Sutani, T. Fukushima, A. Mori, Y. Koshiba, T. Kodani, T. Kanemura, K. Ishida, Improvement of thermal stability of an organic pyroelectric infrared sensor with Parylene C coating, *Jpn. J. Appl. Phys.* 59 (2020) SGGG05, <https://doi.org/10.7567/1347-4065/ab5d70>.
- [34] Karakurt, I.; Zhong, J.; Lin, L. In 3D printed flexible triboelectric energy harvesters via conformal coating of parylene AF4, MEMS 2019, IEEE: 2019; pp 954–957.
- [35] C. Lagomarsini, C. Jean-Mistral, A. Kachroudi, S. Monfray, A. Sylvestre, Outstanding performance of parylene polymers as electrets for energy harvesting and high-temperature applications, *J. Appl. Polym. Sci.* 137 (2020), 48790, <https://doi.org/10.1002/app.48790>.
- [36] H.-w. Lo, Y.-C. Tai, Parylene-based electret power generators, *J. Micromech. Microeng.* 18 (2008), 104006, <https://doi.org/10.1088/0960-1317/18/10/104006>.
- [37] Z. Liu, M. Muhammad, L. Cheng, E. Xie, W. Han, Improved output performance of triboelectric nanogenerators based on polydimethylsiloxane composites by the capacitive effect of embedded carbon nanotubes, *Appl. Phys. Lett.* 117 (2020), 143903, <https://doi.org/10.1063/5.0025001>.
- [38] B. Fan, Y. Liu, D. He, J. Bai, Achieving polydimethylsiloxane/carbon nanotube (PDMS/CNT) composites with extremely low dielectric loss and adjustable dielectric constant by sandwich structure, *Appl. Phys. Lett.* 112 (2018), 052902, <https://doi.org/10.1063/1.5016543>.
- [39] J.-W. Lee, W. Hwang, Theoretical study of micro/nano roughness effect on water-solid triboelectrification with experimental approach, *Nano Energy* 52 (2018) 315–322, <https://doi.org/10.1016/j.nanoen.2018.08.008>.
- [40] M.P. Kim, Y. Lee, Y.H. Hur, J. Park, J. Kim, Y. Lee, C.W. Ahn, S.W. Song, Y.S. Jung, H. Ko, Molecular structure engineering of dielectric fluorinated polymers for enhanced performances of triboelectric nanogenerators, *Nano Energy* 53 (2018) 37–45, <https://doi.org/10.1016/j.nanoen.2018.08.032>.
- [41] J. Kim, S.C. Jang, K. Bae, J. Park, H.-D. Kim, J. Lahann, H.-S. Kim, K.J. Lee, Chemically tunable organic dielectric layer on an oxide TFT: poly (p-xylylene) derivatives, *ACS Appl. Mater. Interfaces* 13 (2021) 43123–43133, <https://doi.org/10.1021/acsami.1c13865>.
- [42] J. Lahann, Reactive polymer coatings for biomimetic surface engineering, *Chem. Eng. Commun.* 193 (2006) 1457–1468, <https://doi.org/10.1080/00986440500511619>.
- [43] J. Gao, T. Chen, C. Dong, Y. Jia, P.-I. Mak, M.-I. Vai, R.P. Martins, Adhesion promoter for a multi-dielectric-layer on a digital microfluidic chip, *RSC Adv.* 5 (2015) 48626–48630, <https://doi.org/10.1039/C5RA08202A>.
- [44] C. Hassler, R.P. von Metzen, P. Ruther, T. Stieglitz, Characterization of parylene C as an encapsulation material for implanted neural prostheses, *J. Biomed. Mater. Res. Part B* 93B (2010) 266–274, <https://doi.org/10.1002/jbm.b.31584>.



Minsoo P. Kim is currently an assistant professor in Chemical Engineering at Sunchon National University. He received his Ph.D. in Chemical and Biomolecular Engineering from Korea Advanced Institute of Science and Technology (KAIST) in 2014. He worked as a postdoctoral fellow in School of Chemical Engineering at Sungkyunkwan University from 2014–2015 and subsequently, in Department of Chemistry at New York University from 2015–2016. From 2016 to 2023, he held the position as a research professor at Ulsan National Institute of Science and Technology (UNIST). His research interests are in the area of functional nanostructured materials for flexible electronics, sensors, and energy devices.



Gunoh Lee is currently a graduate student in integrated PhD course in Department of Chemical Engineering and Applied Chemistry at Chungnam National University. He received his BS in Department of Chemical Engineering and Applied Chemistry at Chungnam National University in 2021. His research interests are in the area of functionalized Parylene-based polymer thin film for the application of future electronics.



Byeongil Noh is currently a graduate student in Master course in Department of Chemical Engineering and Applied Chemistry at Chungnam National University. He received his BS in Department of Chemical Engineering and Applied Chemistry at Chungnam National University in 2023. His research interests are in the area of functionalized Parylene-based polymer thin film for the application of future electronics.



Jaehyun Kim received his MS in Department of Chemical Engineering and Applied Chemistry in 2022, and BS in Department of Fine Chemical Engineering and Applied Chemistry at Chungnam National University in 2020. His research interests are in the area of functionalized Parylene-based polymer thin film for the application of future electronics.



Prof. Kyung Jin Lee is currently a professor in Department of Chemical Engineering and Applied Chemistry at Chungnam National University. He received his PhD in School of Chemical and Biological Engineering in 2009 and BS in School of Chemical Engineering in 2003 at Seoul National University. From 2009 to 2012, he worked at University of Michigan, Ann Arbor as a postdoctoral associate in the Department of Chemical Engineering. His research are in the area of the preparation of functionalized polymer and its application for electronics, sensors, and energy devices.



Min Sub Kwak is currently a Ph.D. student in Chemical Engineering at Ulsan National Institute of Science and Technology (UNIST). He received his M.S. in Electronic Materials Engineering from Korea Maritime and Ocean University (KMOU) in 2022. He worked as researcher in School of Materials Science and Engineering at Pukyong National University from 2022-2023. His research interests are in the area of functional nanostructured materials for wearable electronics, sensors, and energy harvestings.



Prof. Hyunhyub Ko is currently a professor in Energy and Chemical Engineering at Ulsan National Institute of Science and Technology (UNIST). He received his PhD in Materials Science and Engineering from Georgia Institute of Technology in 2008, MS in Materials Science and Engineering from Iowa State University in 2004, MS in Chemical Engineering from Yonsei University in 2001, and BS in Chemical Engineering from Chung-Ang University in 1999. From 2008 to 2010, he worked at University of California, Berkeley as a postdoctoral fellow in the department of Electrical Engineering and Computer Sciences. His research interests are in the area of functional nanomaterials for flexible electronics, sensors, and energy devices